Oral Reference: ICF131

SHORT FATIGUE CRACK GROWTH UNDER MULTIAXIAL NONPROPORTIONAL LOADING

J. HOFFMEYER [1], R. DÖRING [2], T. SEEGER [1] AND M. VORMWALD [2]

[1] Fachgebiet Werkstoffmechanik, TU Darmstadt, 64287 Darmstadt, Germany
[2] Institut für Strukturmechanik, Bauhaus-Universität Weimar, 99421 Weimar, Germany

ABSTRACT

Initiation and growth of short fatigue cracks under nonproportional cyclic push-pull and torsion loading have been investigated. The final aim is the improvement of the accuracy of lifetime prediction. The crack growth has been studied experimentally using the plastic replica technique in the length range from 5µm to 500µm. More than 95% of the fatigue life is governed by short fatigue crack growth. A critical plane approach based on elastic-plastic fracture mechanics is used to model the fatigue process. A Paris-type crack growth law, using the effective cyclic J-integral ΔJ_{eff} and a mixed mode criterion, is integrated to give crack growth curves. The J-integral and crack opening stresses and strains are calculated with approximation equations. Stress-strain paths are predicted using the plasticity model of Jiang [1]. The agreement between model and real damage evolution is shown comparing experimentally determined crack growth curves, cracking directions and life curves for the materials S460N and Al 5083.

KEYWORDS

fatigue, short cracks, multiaxial nonproportional loading, lifetime prediction, mixed mode, cyclic plasticity

INTRODUCTION

For metallic materials the number of cycles to initiate a fatigue crack of technical size of about 0.5mm is determined by the growth of short cracks [2]. Therefore, the fatigue process can be successfully modelled based on fracture mechanics. A significant improvement of lifetime predictions for uniaxial [3, 4] and proportional multiaxial [5, 6] variable amplitude loading has been achieved applying such concepts. Based on this the crack nucleation and the stage of short fatigue crack growth under nonproportional multiaxial loading is investigated and modelled here. The model is described and its accuracy is examined.
Fatigue cracks often nucleate in areas close to the surface where the crystalline microstructure exhibits minor microscopic defects. In metallic alloys these are usually inclusions or surface defects from the manufacturing process. In pure or smoothly finished materials crack nucleation may arise from intrusions and extrusions resulting from micro-plastic deformations. An overview is given for example by Suresh [2] or McDowell [7], with special reference to multiaxial loading by Socie and Marquis [8]. For the microcrack growth, following the microcrack nucleation, the stages I and II are distinguished. During stage I the growth is determined by the maximum shear stress amplitudes. Dependent on the microstructure and the amplitudes a change of the crack growth plane occurs into the direction perpendicular to the maximum normal stress amplitude (stage II). The phase of crack nucleation, the stage I and II short crack growth is illustrated in damage maps by Socie and Marquis [8]. Nucleation, stage I and early stage II crack growth is influenced by

the microstructure. Models describing such effects are published for uniaxial or proportional multiaxial loading. An extension to nonproportional cases has been recently proposed by Suhartono [9]. It is based on a concept proposed by Socie und Furman [10]. Beyond this, more than 100 hypotheses for lifetime prediction under multiaxial cyclic loading have been published during the last decade. A survey of the current state of the art can be found in [8]. The hypotheses can be divided into stress, strain, energy and fracture mechanics based models. The concept proposed in this paper belongs to the latter.

MATERIAL DATA AND EXPERIMENTAL PROCEDURE

The materials investigated are the fine grained steel S460N (E = 208500 MPa, $R_{p0.2}$ = 500 MPa, R_m = 643MPa) and the aluminium alloy Al 5083 (E = 68000 MPa, $R_{p0.2}$ = 169 MPa, R_m = 340 MPa). The steel shows a cyclic hardening for high and softening for low strain amplitudes. Al 5083 exhibits cyclic hardening and behaves linearly-elastically except for very high strains. The material properties are described in detail by Savaidis [6]. The multiaxial tests have been performed on unnotched thin-walled tube specimens. The internal diameter is 36 mm, the wall thickness 2.5 mm. Standard hourglass shaped specimens (diameter 6 mm) have been used for uniaxial tests and for the identification of the material parameters of the plasticity model. The tests have been conducted on a hydraulic tension-torsion machine at room temperature under strain control. For further details see [5, 11]. Damage mechanisms and the lives have been investigated under in-phase and 45º and 90º out-of-phase constant amplitude loading. Life to technical crack size, cyclic deformation behaviour, short crack growth and crack closure have been determined. During some of the tests replicas have been taken to examine the nucleation and growth of short cracks. Crack growth could thus be traced back to 2-10µm surface crack length. For the examination of crack closure replicas have been taken at different positions of one hysteresis loop in 90º out-of-phase tests [11].

MODELLING OF FATIGUE CRACK GROWTH

A reliable model for the calculation of stress-strain paths is a prerequisite for an accurate lifetime prediction. Therefore, Jiang`s plasticity model [1] is used here. Details of its application may be found elsewhere [Hof00]. The model proposed in the following is used to calculate the crack growth of short fatigue cracks applying fracture mechanics. Simplifying assumptions had to be made for such a model as outlined below:
1. The directions of the principal axes are not constant under nonproportional multiaxial loading. The critical plane is determined iteratively by carrying out the calculations for each potential direction. The plane with the highest crack growth rate is regarded as the critical one.
2. As there are no closed hysteresis loops the usual rainflow cycle counting has to be substituted. It is modified in the way that the stresses and strains perpendicular to the plane under consideration are treated as primary damage variable as described in [12].
3. A semi-circular surface crack of the initial length a_0 is assumed that keeps its direction and remains in its plane. The quantity a_0 is determined from the strain life curve of uniaxial experiments by resolving the crack growth law in terms of a_0. The growth of a single crack is modelled. The influence of crack coalescence and changes from stage I to II are – in case of occurrence – only included in an averaging way by the initial crack length a_0 .
Because the requirements for applying linear-elastic fracture mechanics are not fulfilled for short cracks elastic-plastic parameters have to be applied. The crack growth rate is described by a Paris-type law using an effective, that means crack closure adjusted cyclic crack tip parameter, eqn. (1). The approximation equation for the cyclic J-integral ΔJ according to Dowling [13] is used. For nonproportional multiaxial loading the equation has to be modified to consider the mixed mode situation, i.e. the combination of crack opening mode I and plane shear mode II, eqn. (2) and (3). Life (to cracks of technical size) is defined as the number of cycles calculated from the fictitious initial crack length a_0 to a = 250µm.

$$\frac{\mathrm{d}a}{\mathrm{d}n} = C\left(\Delta J_{\mathrm{eff}}\right)^m \qquad (1) \quad ; \quad \Delta J_{\mathrm{eff}} = \Delta J_{\mathrm{I,eff}} + \Delta J_{\mathrm{II,eff}} \qquad (2)$$

$$\Delta J_{I,eff} = \left(1.24 \cdot \frac{\left(\Delta\sigma_{eff}\right)^2}{E} + 1.02 \cdot \frac{\Delta\sigma_{eff} \cdot \Delta\varepsilon_{p,eff}}{\sqrt{n'}} \right) \cdot a \quad , \quad \Delta J_{II,eff} = \left(1.24 \cdot \frac{\left(\Delta\tau_{eff}\right)^2}{G} + 1.02 \cdot \frac{\Delta\tau_{eff} \cdot \Delta\gamma_{p,eff}}{\sqrt{n'}} \right) \cdot a \tag{3}$$

The index „p“ indicates plastic deformation, E, G and n' are Young's and shear modulus and the cyclic hardening exponent. As a mixed mode state occurs at the crack tip an equivalent quantity has to be derived from the mode-separated parameters. For static and proportional cyclic loading a number of mixed mode fracture criteria have been derived (for long cracks). However no comparable criteria are known to the authors for nonproportional cyclic loading, particularly in the realm of elastic-plastic fracture mechanics. Therefore, the J-integrals are simply added in the model, eqn. (2), yielding capabilities to improvements by results of further research on this topic.

Crack closure is considered as an essential aspect because it explains sequence effects for service loads [3]. In the model it is supposed to be responsible for sequence effects, the description of the mean stress dependency, and the ratio of multiaxiality $\lambda=\sigma_2/\sigma_1$. Crack opening stresses are estimated using an equation originally proposed by Newman [14], eqn. (4), for long cracks, which is modified and extended here by certain terms to improve and include the effects mentioned above.

$$\sigma_{op} = \begin{cases} \sigma_O \cdot \left(A_0(\lambda) + A_1(\lambda) \cdot R + A_2(\lambda) \cdot R^2 + A_3(\lambda) \cdot R^3 + c_\lambda(\lambda) \right) & \text{for } \sigma_{\min}/\sigma_{\max} > 0 \\ \sigma_O \cdot \left(A_0(\lambda) + A_1(\lambda) \cdot R + c_\lambda(\lambda) \right) & \text{for } \sigma_{\min}/\sigma_{\max} \le 0 \end{cases} \tag{4}$$

$$A_0(\lambda) = 0{,}535 \cdot \cos\left(\frac{\pi}{2} \cdot \frac{\sigma_O}{\sigma_F(\lambda)} \right) + a_{\mathrm{mitt}}(\lambda) \quad ; \quad A_1(\lambda) = 0{,}344 \cdot \frac{\sigma_O}{\sigma_F(\lambda)} + a_{\mathrm{mitt}}(\lambda);$$

$$A_3 = 2 \cdot A_0 + A_1 - 1; \quad A_2 = 1 - A_0 - A_1 - A_3; \quad c_\lambda(\lambda) = 0{,}535 \cdot \cos\left(\frac{\pi}{2} \frac{\sigma_w(\lambda)}{\sigma_F(\lambda)} \right) - 0{,}344 \cdot \frac{\sigma_w(\lambda)}{\sigma_F(\lambda)} + \frac{\Delta\sigma_o}{\sigma_w(\lambda)} - 1$$

$$\sigma_F(\lambda) = \frac{\sigma_F}{\sqrt{1-\lambda+\lambda^2}}, \qquad \sigma_w(\lambda) = \frac{\sigma_w}{\sqrt{(1+\lambda)^2 - \left(\frac{\sigma_w}{\tau_w}\right)^2 \cdot \lambda}}, \qquad \sigma_{sch}(\lambda) = \frac{\sigma_{sch}}{\sqrt{(1+\lambda)^2 - \left(\frac{\sigma_{sch}}{\tau_{sch}}\right)^2 \cdot \lambda}}$$

$$a_{\mathrm{mitt}}(\lambda) = 1 - 0.535\cos\left(\frac{\pi}{2} \frac{\sigma_{sch}(\lambda)}{\sigma_F(\lambda)} \right) - \frac{\sigma_w(\lambda)}{\sigma_{sch}(\lambda)} \left[1 + 0.344 \frac{\sigma_w(\lambda)}{\sigma_F(\lambda)} - 0.535\cos\left(\frac{\pi}{2} \frac{\sigma_w(\lambda)}{\sigma_F(\lambda)} \right) + c_\lambda(\lambda) \right]$$

$\sigma_F(\lambda)$ is a fictitious yield stress in terms of λ, $\sigma_w(\lambda)$ is the endurance limit (for $R=\sigma_{min}/\sigma_{max}=-1$) under uniaxial loading, $\sigma_{sch}(\lambda)$ is the corresponding endurance limit for R=0. Thus, the mean stress dependency is taken into account via σ_w and σ_{sch}, the effect of the ratio of multiaxiality enters the equation via the shear endurance limits for R=-1 and R=0, respectively.

For shear stress dominated cycles the roughness of the crack flanks is the most important quantity. This is not yet described by the model. It is assumed that shear stresses can only act at the crack tip when the crack is opened by mode I loading. When the crack is closed the tip is protected by friction and surface contact. Experimental investigations on crack opening behaviour support this idea, but there is a continuous transition between completely closed and completely opened crack.

RESULTS: CRACK GROWTH CURVES, CRACK ANGLES AND STRAIN LIFE CURVES

Replicas taken during some of the tests have been examined by scanning electron microscopy yielding series of crack pictures, fig. 1, and crack growth curves, fig. 2. Microcracks could be found already after 2-5% of lifetime. This means that nucleation of critical cracks is completed in a very early stage of fatigue. This justifies its neglecting in the model. As mentioned this portion of fatigue life is implicitly considered by the starting crack length a_0.

Cracks were traced back to ranges under 10 µm. For all investigated loading cases and crack modes the characteristic growth of short cracks, e.g. [7], was observed. Microcracks grow fast under accelerations and decelerations, followed by a stage of slower growth and finally the crack length increases dramatically. The data of table 1 together with the load sequences form the input data for the calculations. For S460N the plasticity model was applied. For Al 5083 linear-elastic deformation was assumed.
For both materials the crack growth curves for 90º and 45º out-of-phase loading can be described well by the model, fig. 2. For torsion with a superimposed static normal stress the calculation is slightly conservative for S460N. There are noticeable effects of deceleration of crack growth for S460N, especially under torsion loading indicating roughness induced closure. Generally only between 3 and 5 cracks could be detected. Their distance was too large to cause any interaction.

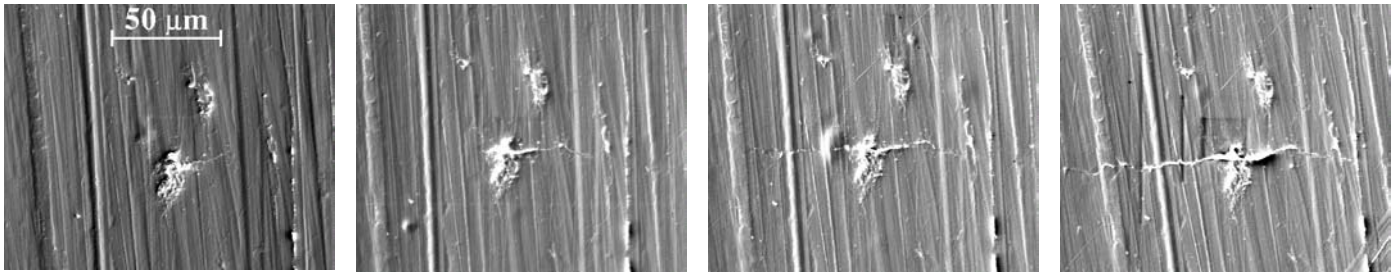

n = 1512 n = 3500 n = 8507 n = 17011

Figure 1: Short crack; Al 5083; ε_a=0.231%; γ_a=0.4%; 90° out-of-phase loading; life to failure: 26000 cycles

Table 1. Input data for the short crack growth model

Material	C [mm/cyc. (N/mm)$^{-m}$]	m [-]	$\Delta K_{th,\,eff}$ [MPa·mm$^{1/2}$]	σ_w [MPa]	τ_w [MPa]	$\Delta\sigma_{sch}/2$ [MPa]	σ_F [MPa]	a_0 [µm]
Al 5083	$2\cdot10^{-4}$	1.55	28	180	105	130	352	25
S460N	$3.9\cdot10^{-5}$	1.575	110	340	200	245	432	33

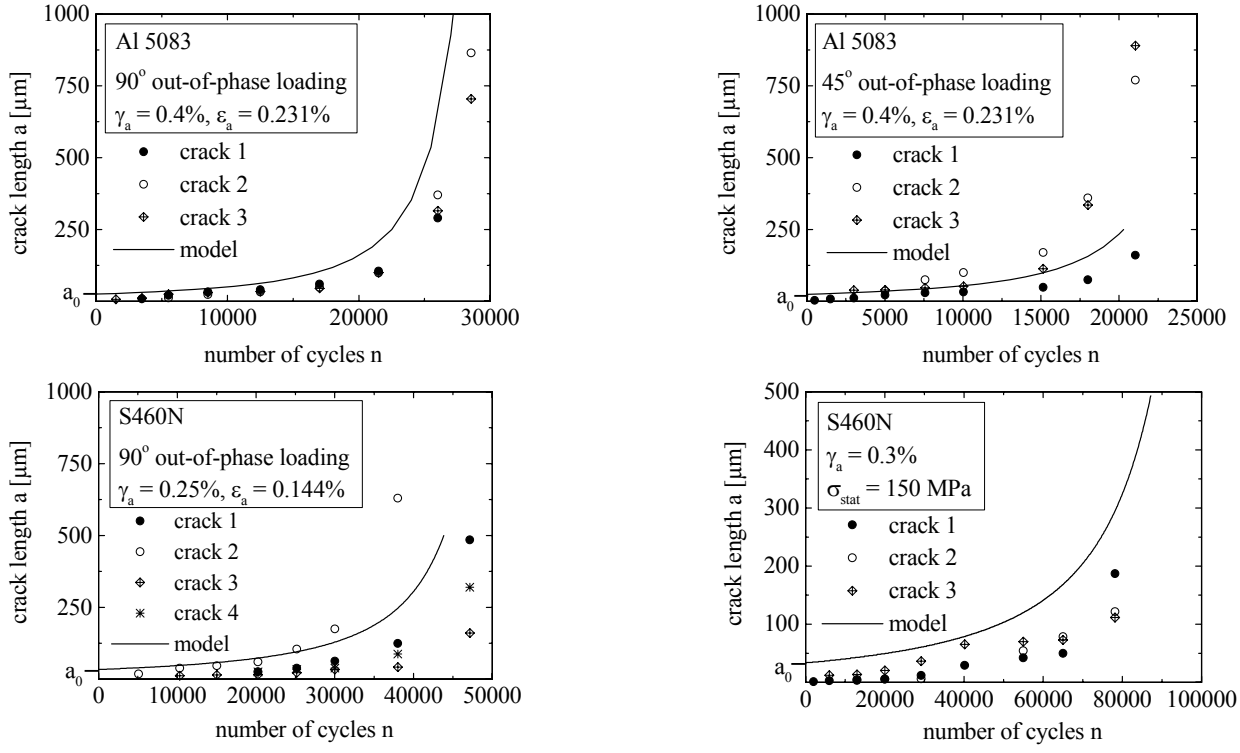

Figure 2: Comparison of short crack growth curves, calculated and determined by replicas

As the critical plane is determined by iteration, angles of surface cracks are obtained by the simulations. The orientations give information about the crack mode and are basis for the choice of crack driving force pa-

rameters. Under push-pull and proportional loading short cracks grew as mode I cracks perpendicular to the maximum principal stress amplitude, under torsion in the directions of the maximum shear stress amplitude [Sav97]. Experimental results for out-of-phase loading show clearly the good correlation between simulation, where mode I driven growth is assumed, and experiment, fig. 3 and 4. For S460N cracks angles of 5° to 25° were measured in the very early stage of crack growth. For longer cracks a value of 20° was found, fig. 3. The calculation yields a constant value of 19°. For out-of-phase loading the model describes no dependency of the angles on the crack length but on plastic deformations. For elastic material behaviour, as assumed for the Al 5083, an angle of 0° is calculated for 90° out-of-phase loading. At higher (plastic) amplitudes the angle is supposed to increase similar as for the steel. For Al 5083 crack angles of 4° were found in the very early stage in this experiment. The orientation changes with the growing crack to 15°, fig. 4. Reason for deviations could be plastic deformations. Under 45° out-of-phase loading values from 30° to 50° have been measured, the simulation yields 25°. For proportional loading angles of 30° to 50° have been determined in the experiment and 26° in the calculation.
The microcracks and short cracks usually did not change their orientation. If however this change occurred, it happened continuously. No distinct kinks as a consequence of a transition from mode II to mode I have been observed. This justifies the model assumption that cracks remain plane. The results are accurate if mode I controlled crack growth occurs. For shear mode crack growth, as observed under pure cyclic torsion, deviations arise because its accurate consideration would require an extended crack growth criterion.

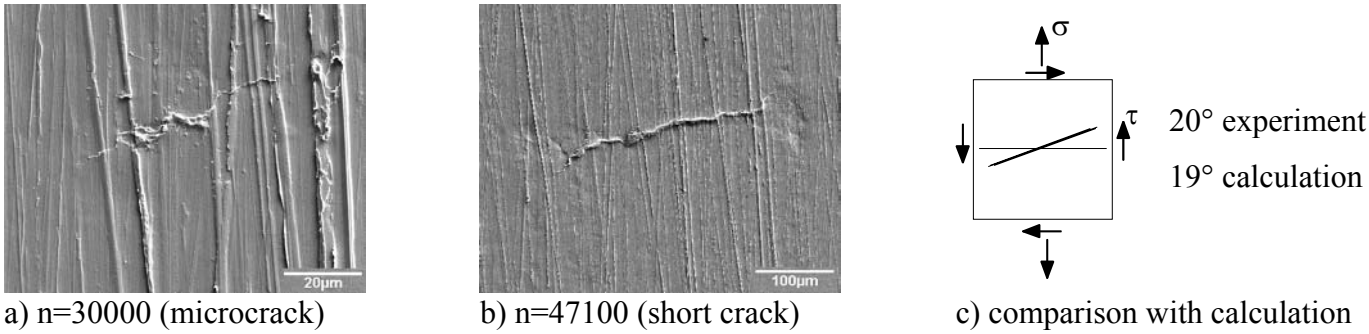

a) n=30000 (microcrack) b) n=47100 (short crack) c) comparison with calculation

Figure 3: Crack angles: a) microcrack and b) short crack (S460N; 90° out-of-phase loading; $\varepsilon_a = 0.144\%$, $\gamma_a = 0.25\%$; polishing marks in direction of specimen axis)

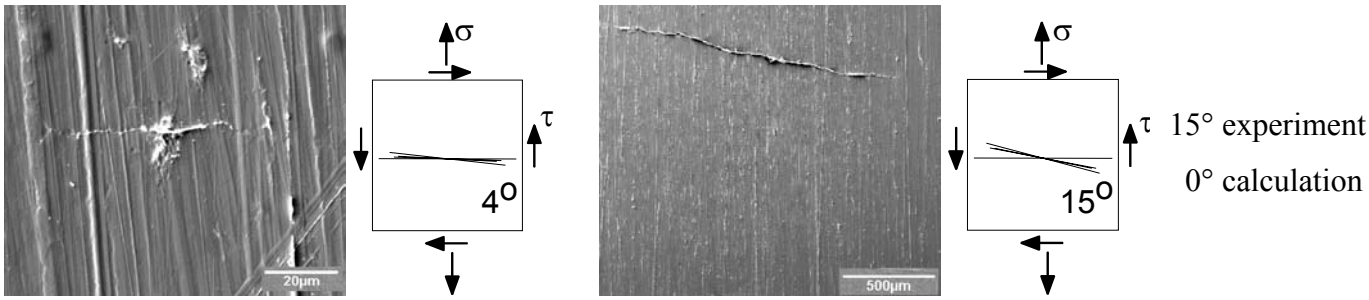

a) n=12500 (microcrack) b) n=28500 (crack of technical size)

Figure 4: Crack angles: a) microcrack and b) crack of technical size (Al 5083, 90° out-of-phase loading, $\varepsilon_a = 0.231\%$, $\gamma_a = 0.4\%$)

Under 45° and 90° out-of-phase loading for both materials the fatigue life is slightly shorter compared to proportional loading, fig. 5. For all phase-shifts the simulated lives agree well with the experimentally determined lives for S460N. The lifetime prediction results tend to slightly underestimate lives except for severe plastic deformations under 90° out-of-phase loading. In the simulations and experiments the strain life curves for 45° and 90° phase-shifts are close together. The conspicuous convolution of the strain life curve for 90° out-of-phase loading results from the determination of the critical plane that changes with higher amplitudes. Cross-hardening is not considered in the plasticity model. This might lead to deviations in the lifetime prediction. Also for Al 5083 the calculations give accurate results for all phase-shifts. Under 90° out-of-phase loading calculated lives agree with the experimentally determined lives as shown for S460N. At the highest strain plastic deformations ought to be considered. Also for Al 5083 the strain life curves for

45° and 90° phase-shifts are close together in the simulation and experiment. By using a mixed mode criterion and plasticity including cross-hardening further improvements could be achieved.

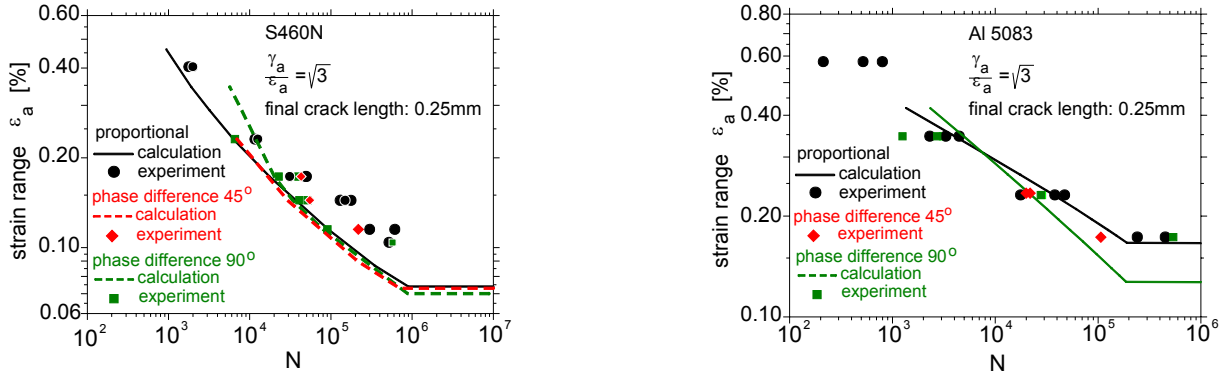

Figure 5: Strain life curves: Influence of out-of-phase loading on fatigue life and comparison of calculated and experimentally determined lives for S460N (a) and Al 5083 (b)

SUMMARY

The proposed concept can be used to calculate the growth of short fatigue cracks to technical size under nonproportional multiaxial loading with good to acceptable accuracy. The agreement of the theoretical perceptions as stated in the model with the real damage behaviour was shown by comparisons of calculated and experimentally determined crack growth curves, crack directions and life curves. Jiang's plasticity model is employed to describe the plastic deformation behaviour. Crack growth in a critical plane is computed from a Paris-like crack growth law using the cyclic J-integral for mixed-mode loading including crack closure. The essential damage mechanisms and quantities that influence the fatigue life are considered. Further investigations regarding mode II crack growth, mixed mode criteria and crack closure will be necessary for improving the lifetime prediction. For the moment the model is not intended to explicitly describe influences of the microstructure, coalescence, microcrack initiation and stage I crack growth, and crack growth at notched components.

ACKNOWLEDGEMENT

Grant support from the „Deutsche Forschungsgemeinschaft“ is gratefully acknowledged.

REFERENCES

1. Jiang, Y. (1993). PhD. Thesis, University of Illinois at Urbana-Champaign.
2. Suresh, S. (1993). *Material Science and Technology*, 6, 509.
3. Vormwald, M. (1989). PhD. Thesis, TH Darmstadt.
4. Vormwald, M.; Heuler, P. and Krae, C. (1994). In: *ASTM STP 1231*, pp. 221-240, West Conshohocken.
5. Savaidis, G. (1995). PhD. Thesis, TH Darmstadt.
6. Savaidis, G. and Seeger T. (1997). In: *Proceed. of the 5th Int. Conf. On Biaxial/Multiaxial Fatigue and Fracture*, Volume I, pp.81-98, Cracow.
7. McDowell, D.L. (1996). *Int. Journ. Fracture*, 80, 103.
8. Socie, D. F. and Marquis, G.B. (2000). *Multiaxial Fatigue*. SAE Warrendale, ISBN 0-7680-0453-5.
9. Suhartono, H.A. (2000). PhD. Thesis, TU Clausthal.
10. Socie, D. F. and Furman, S. (1996). In: *Fatigue 96, Proc. 6th Int. Fat. Congress*, pp. 967, Lütjering, G., Nowack, H. (Eds.), Elsevier, Oxford.
11. Hoffmeyer, Döring, Schliebner, Vormwald, Seeger. (2000). *Report FD-04/2000*, TU Darmstadt.
12. Bannantine, J.A. and Socie, D.F. (1989). In: *3rd Int. Conf. biaxial/multiaxial fatigue*, pp. 12ff, Stuttgart.
13. Dowling, N.E. and Begley, J.A (1976). In*: Mechanics of crack growth, ASTM STP 590*, pp. 82-103.
14. Newman, J.C. Jr. (1984). *Int. Journ. Fracture*, 24, R131.